

## Particle Diffusion in a Meandering Jet

STEPHANIE DUTKIEWICZ,<sup>1</sup> ANNALISA GRIFFA, AND DONALD B. OLSON

*Rosenstiel School of Marine and Atmospheric Science, University of Miami, Miami, Florida*

The process of turbulent mixing across an ideal model of a meandering Gulf Stream is studied considering particle motion in two dimensions. The turbulent motion is modeled using a "random flight" model that assumes that the evolution of the turbulent velocity along trajectories is a Markov process, with the velocity at one time step depending linearly on the velocity at the previous step. This turbulent field is superimposed on a meandering jet (similar to the one considered by Bower (1991)) propagating steadily eastward. In Bower's model the particles are constrained to move along streamlines in the translating frame; in our model the turbulent motion allows the particles to cross streamlines, resulting in an exchange between the different regions of the flow. The major exchange occurs between the "jet core" region and the "recirculating" regions moving with the meanders. Particles launched in the jet core tend to be lost from the jet in plumes at the extrema of the meanders and to be entrained in successive recirculation regions. When in the recirculation regions, particles tend to be trapped and homogenized. The exchange between the jet and the "far field" depends only on diffusion mechanisms and is small for the short integration time considered. An application of the kinematic techniques considers the distribution of biological species across the jet. The tendency for "patches" of organisms to develop in the recirculation regions is observed. In a two-species case, where the species have affinities for the environment on opposite sides of the jet, there is a linear change in species composition across the jet. Patches forming on either side of the jet consist of an admixture of the two species, with the population for the crest or trough environment dominating.

### 1. INTRODUCTION

The Gulf Stream is a strong current jet dividing two different bodies of water, warm saline water of the Sargasso Sea and cool fresh Slope Water (Plate 1). An issue addressed by several authors in the literature [e.g., Bower *et al.*, 1985] concerns the amount of mixing and diffusion that occurs across the Gulf Stream. This is a relevant question from both the physical and the biological points of view, since the Sargasso Sea and the Slope Water differ not only in physical characteristics such as temperature and salt but also in biological properties such as zooplankton and nekton biomass and speciation.

Several studies have shown the existence of a mechanism of mixing which relates the occurrence of meanders to cross-stream motion of fluid parcels [e.g., Owens, 1984; Bower and Rossby, 1989]. A simple kinematic model able to explain at least part of this mechanism and considering the motion of particles in a two-dimensional meandering jet steadily propagating eastward has been proposed by Bower [1991]. While the Bower model shows the mixing process qualitatively, it lacks some important elements to effectively describe diffusion of particles across the stream. One limitation is that the representation of the meandering jet given by Bower does not allow time evolution of the meander shape, which is likely to be an important factor in influencing particle behavior [Bower and Rossby, 1989]. An implementation of the model in this direction has been proposed by Samelson [1992], who considers the effects of harmonic time-dependent fluctuations of the velocity field. Technically, the introduction of the time dependence can give rise to the phenomenon of "deterministic diffusion." Another

limitation of Bower's model (and of Samelson's) is that the particle motion is considered as a strictly deterministic process due solely to the advection of the large-scale velocity of the meandering jet. The action of small-scale turbulence, an important factor in the Gulf Stream [Bower *et al.*, 1985; Lambert, 1982], is not included. This limitation and the questions that it leaves open provide the motivation and the starting point of the present work.

The aim of this paper is to provide a description and an understanding of the turbulent mixing processes associated with the meanders of the Gulf Stream and of the corresponding diffusion of tracers. We concentrate on synoptic time and space scales that are characteristic of the life of the meanders. We implement a simple model of a meandering jet similar to Bower's [1991] by adding to the deterministic velocity field that represents the stream an additional velocity field representing the action of the small-scale turbulence. The motion of the particles in the turbulent jet is studied numerically. A large number of particle trajectories are simulated, and diffusion processes are studied by considering the concentration of the particles in space. In all but one of the experiments, the parameters of the deterministic jet do not change in time, so that the deterministic motion is regular and the diffusion is due solely to the stochastic (turbulent) motion. Only in one experiment, representing a growing meander, is the possible interaction between stochastic and deterministic diffusion considered.

The method that we use to represent the turbulent velocity field superimposed on the jet belongs to a class of so-called "random flight" models [e.g., van Dop *et al.*, 1985; Thomson, 1987]. These models have been successfully applied to estimate pollutant dispersion in the atmosphere [Thomson, 1986], and they have proven to be a simple and flexible tool in the study of complex turbulent flows. Since the particles are assumed to move independently in the flow, the results are applicable only to ensemble or time-averaged diffusion. This is the same limitation as for the method of the advection and diffusion equation, which is often used in the study of

<sup>1</sup>Now at Graduate School of Oceanography, University of Rhode Island, Narragansett.

Copyright 1993 by the American Geophysical Union.

Paper number 93JC01364.  
0148-0227/93/93JC-01364\$05.00

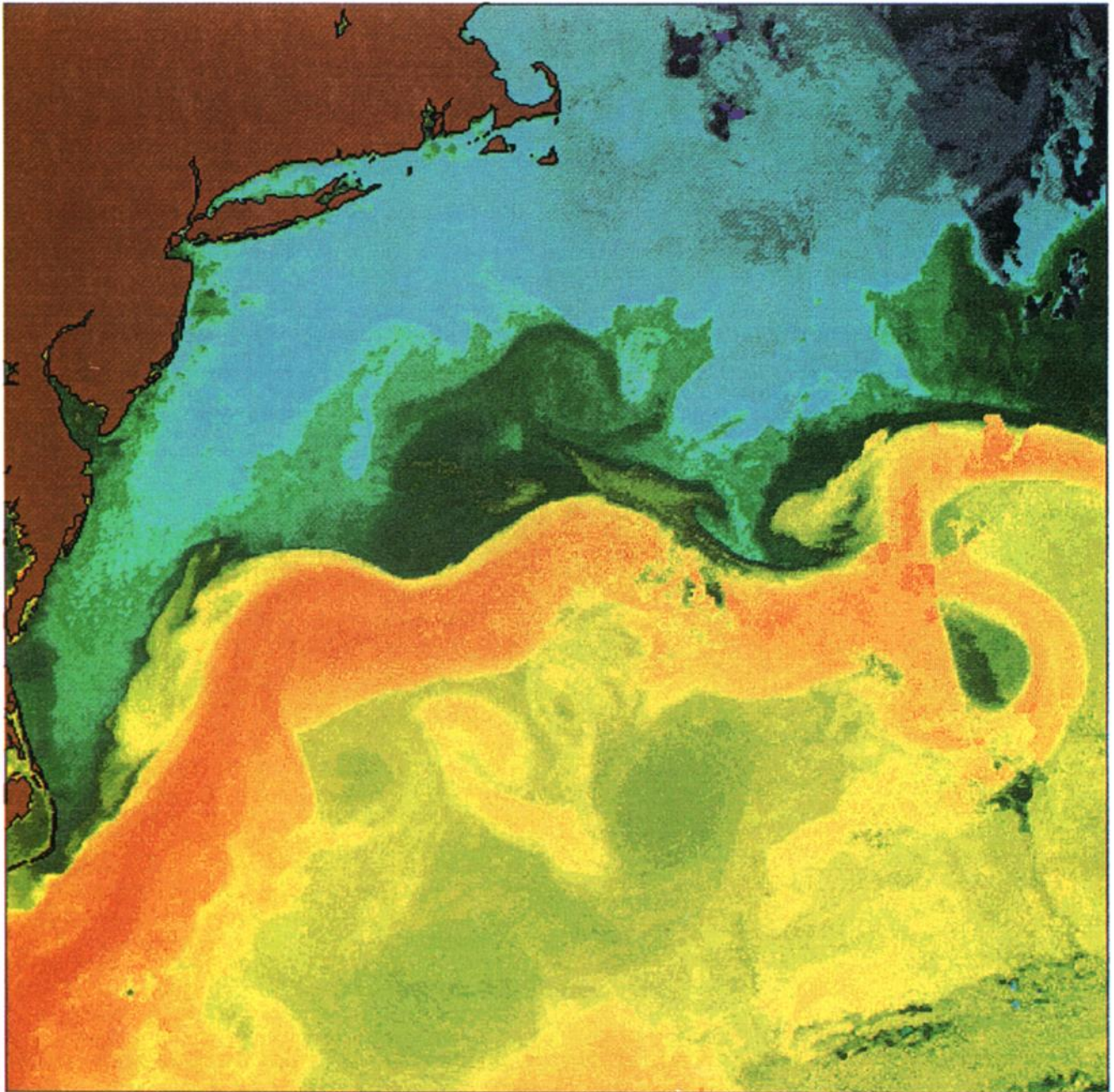


Plate 1. Satellite image of the Gulf Stream. Redder colors indicate warmer water. Image is for April 17, 1989. Data are from NOAA-N advanced very high resolution radiometer.

diffusion. The random flight models, though, appear to be a more powerful method because they can be applied to highly inhomogeneous and nonstationary flows. Finally, the random flight models, being Lagrangian, provide an easy comparison with the float results and allow straightforward calculation of processes such as biological interactions along trajectories.

As an application of a Lagrangian frame computation, we consider the influence of the physical processes of mixing on the characteristics of marine life in systems such as the Gulf Stream. The basic premise is to consider the influence of dispersal in relationship to the cross-stream changes in the environment. The Gulf Stream is at first order a biogeographic boundary with different species occurring on either

side [Grice and Hart, 1962; Wishner and Allison, 1986]. The northern side of the Stream is typically eutrophic, with high phytoplankton and zooplankton biomass and species representative of a transition between subpolar or polar and subtropical biogeographic provinces [Backus, 1986]. On the southern side of the Stream the system is oligotrophic, with a very low biomass made up of subtropical species. As discussed below, meandering and small-scale turbulent diffusion are major sources of patchiness in the biology of the Stream.

In the following section the deterministic velocity field representing a meandering jet similar to that of Bower [1991] is introduced. The representation of the small-scale turbulence superimposed on the jet and its influence on particle

motion are discussed in section 3. In section 4 the results of various numerical experiments are presented, and diffusion patterns and their parameter dependence are explored. The consequences for diffusion of the meander's growth in time are also studied. The application of the kinematic model to parcels containing competing biological species is discussed in section 5.

## 2. JET MODEL: DETERMINISTIC MOTION OF PARTICLES

In this section we introduce the basic form of the kinematic model of the meandering Gulf Stream. The model consists of a two-dimensional meandering jet steadily propagating eastward. A generalization to include meander growth is discussed in section 4.3. Assuming that the flow is nondivergent, the model is written in terms of a stream function in the two-dimensional  $x, y$  plane ( $x$  and  $y$  are cartesian coordinates,  $x$  pointing eastward and  $y$  pointing northward):

$$\psi(x, y, t) = \psi_0 \left( \tanh \left( \frac{\pi}{W} (y - \theta) \right) \right) + \beta \sin(k_y y) \quad (1)$$

where

$\psi_0$  scale factor to determine maximum velocity;

$W$  width of the jet;

$\theta = A \sin k_x(x - ct)$ ;

$A$  amplitude of the meanders;

$k_x = 2\pi/\lambda$ , wavenumber of the meanders;

$c$  phase speed of the meanders;

$\beta$  scale factor to determine the strength of the recirculation;

$k_y = 2\pi/4A$ .

The  $\tanh$  term in (1) keeps the velocity field localized in the  $y$  direction and gives the characteristic jet shape. The term  $\beta \sin(k_y y)$  models the existence of a weak recirculation in the bends of the meanders, as suggested by Gulf Stream models [Ikeda and Apel, 1981] and observations [Cornillon et al., 1986]. Figure 1a shows the stream function over one wavelength for a set of parameter values representative of the Gulf Stream in the midthermocline: 450 km for the wavelength  $\lambda$ , 70 km for the width of the jet  $W$ , 14 km day<sup>-1</sup> for the phase speed  $c$ , and 70 km for the amplitude  $A$ . The scale factors  $\psi_0$  and  $\beta$  are chosen so that the maximum current speed is about 120 cm s<sup>-1</sup> and the maximum recirculation speed in the meander bends is about 1 cm s<sup>-1</sup>. Since the streamlines approximately correspond to the lines of the downstream velocity  $U$  of the current, the two bold streamlines in Figure 1a approximately indicate the region where  $U$  is greater than the phase speed of the meanders  $c$ .

The trajectory  $x(t), y(t)$  of a particle in the field (1), interpreted as a flow on an isopycnal surface, is given by the integration of

$$\begin{aligned} \frac{dx}{dt} &= U = -\frac{\partial \psi}{\partial y} \\ \frac{dy}{dt} &= V = \frac{\partial \psi}{\partial x} \end{aligned} \quad (2)$$

where  $U$  and  $V$  are the  $x$  and  $y$  components, respectively, of the vector velocity  $\mathbf{U}$ . The particle motion is strictly deter-

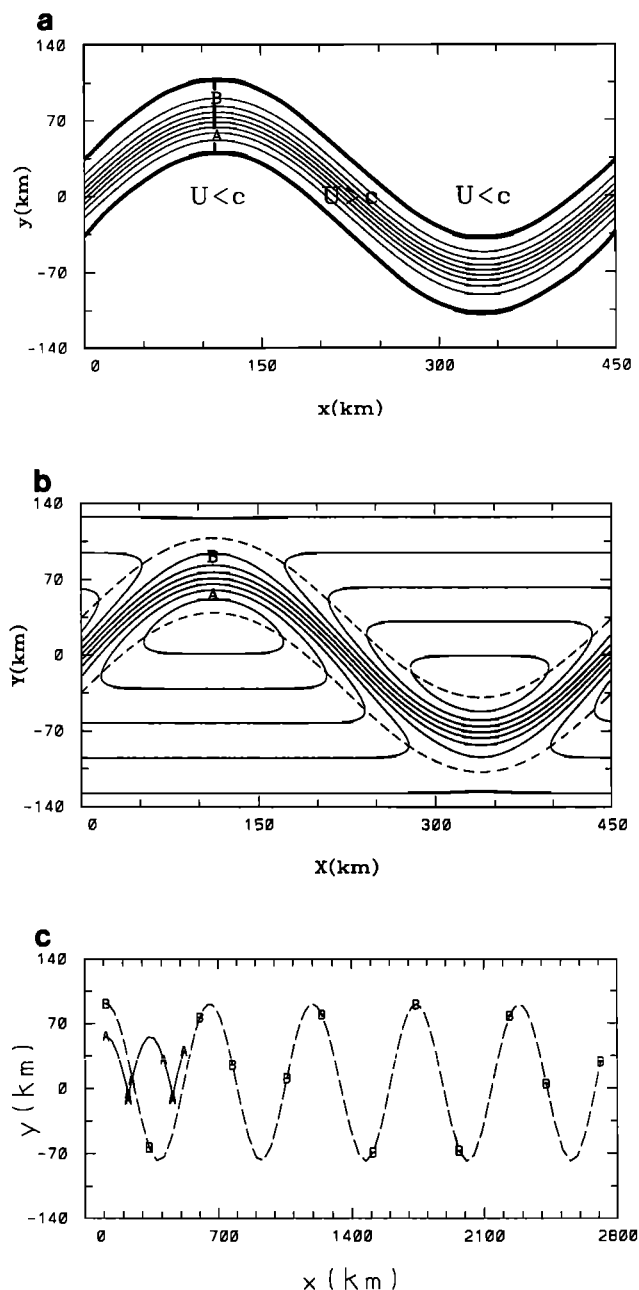


Fig. 1. (a) Stream function  $\psi$  in the fixed reference frame. Area between bold lines is the "jet region," where  $U > c$ . Line across crest and points A and B show cross section and points used in EXP0. (b) Stream function  $\Psi$  in the translating reference frame (solid lines) and stream function  $\psi$  in fixed reference frame (dashed lines). (c) Trajectories in the fixed frame. The symbol A indicates the particle launched at A, in the recirculating region, and B indicates the particle launched at B, in the jet core region. Points for A and B are plotted every  $2\frac{1}{2}$  days out to the meander period,  $T_m = 32$  days.

ministic and depends on the initial conditions  $x(0), y(0)$ . Since the stream function (1) is time dependent, the particles cross streamlines. A simple method of studying this motion without explicitly solving (2) consists in rewriting the stream function in a new coordinate system,  $(X, Y) = (x - ct, y)$ , moving with the phase speed  $c$  [Flierl, 1981]. In this translating frame the stream function is independent of time:

$$\Psi(X, Y) = \psi_0 \left( \tanh \left( \frac{\pi}{W} (Y - \Theta) \right) \right) + \beta \sin(k_y Y) + cY \quad (3)$$

where  $\Theta = A \sin(k_x X)$  and the motion of the particles is along streamlines. Figure 1b shows the stream function (3) over one wavelength. As noted by Bower [1991], there are two types of regions in the meandering jet field (3): (1) regions where the streamlines are closed, in the bends of the meanders, and (2) a region where the streamlines are open, in the center of the stream. The closed streamlines are recirculating regions, in the sense that particles deployed in them recirculate in closed loops when observed from the translating frame. Particles deployed where the streamlines are open, however, move eastward relative to the fixed coordinate frame, progressing in the stream. The open-streamlines region will be indicated as the "jet core region." Notice that, as pointed out by Bower, the motion of the particles appears quite different when observed in the fixed frame (Figure 1c), as can be easily understood by looking at the superposition of the jet in the fixed frame on the stream function (3) (Figure 1b). Particles in the fixed frame appear to cross streamlines and, if initialized in a region of the jet that overlaps a recirculating region, appear to exit and reenter the jet, moving downstream with average speed equal to the phase speed of the meanders.

### 3. TURBULENT MOTION OF THE PARTICLES: RANDOM FLIGHT MODELS

In this section we study the motion of particles in the presence of a turbulent velocity  $\mathbf{u}$  with components  $u$  and  $v$  superimposed on the meandering jet:

$$\begin{aligned} \frac{dx}{dt} &= U + u \\ \frac{dy}{dt} &= V + v. \end{aligned} \quad (4)$$

Before discussing equations (4) in detail, let us make some general remarks. The turbulent velocity  $\mathbf{u}$  is characteristic of the complex and incoherent motions that occur at scales much smaller than the scales of the jet and is described in statistical terms, in contrast to the deterministic large-scale velocity  $U$ . In this paper we focus on the simplest type of particle statistics, i.e., on the statistics that describe the motion of single, independent particles in the flow, as opposed to the more complex statistics relative to simultaneous motion of two or more particles [Davis, 1983; Csányi, 1980]. A complete description of the single-particle statistics for a stationary process is given by  $C(x, y, t, x_0, y_0, 0)$ , the probability density function of a particle being found at position  $x, y$  at time  $t$  when the particle has been deployed at  $x_0, y_0$  at  $t = 0$ . Notice that as a function of  $x, y$ , and  $t$ ,  $C$  can be interpreted as the concentration at time  $t$  of the particles that have been deployed at  $t = 0$  in  $x_0, y_0$  in different realizations of the turbulent flow or alternatively as the normalized mean concentration of a conservative passive tracer that has been instantaneously released at  $t = 0$  from a point source  $x_0, y_0$ . In fact  $C$  is the Green's function for the averaged transport equation [Monin and Yaglom, 1971].

Here equations (4) are solved numerically for a large number of particle trajectories starting from selected initial conditions in the jet. Each particle is simulated independently in a different realization of  $\mathbf{u}$ . The statistics are then computed by averaging over the ensemble of particles with the same initial conditions, and the evolution of the concentration  $C$  is studied by considering the distribution of the particles in space and time.

The turbulent velocity  $\mathbf{u}$  in (4) is described following the method of random flight, i.e., as a purely time-dependent process representing the turbulent velocity field as sampled by the particle during its motion. With respect to other representations of  $\mathbf{u}$  that include the full space dependence (e.g., as a two-dimensional  $(x, y)$  stochastic Fourier series [Davis, 1991]), the present method allows for a substantial economy in computing time and in information about the turbulent field while still retaining the necessary ingredients to describe single-particle turbulent diffusion. In the following, we briefly summarize the basic characteristics of the random flight models. For a more complete overview, see Pasquill and Smith [1983].

Consider first the simplest case of a one-dimensional, homogeneous, and stationary turbulent field with no mean shear. In this case the turbulent velocity  $u(t)$  is simply described by the Langevin [1908] equation

$$du = (-uFdt) + d\mu \quad (5)$$

and  $x(t)$  is given by

$$dx = udt$$

where  $F = 1/T_L$  is the inverse of the constant time scale  $T_L$  over which the particle velocity is correlated,  $d\mu$  is a random increment from a normal distribution with zero mean and second-order moment  $\langle d\mu \cdot d\mu \rangle = (2\sigma/T_L)dt$ , and  $\sigma$  is the constant fluid velocity variance.

Equation (5) describes  $u(t)$  as a Markovian process, where the velocity at one time step depends linearly on the velocity at the previous time step [Hanna, 1979]. Physically, (5) indicates that when a particle moves through the fluid, it loses a fraction of its momentum  $dt/T_L$  to the surrounding fluid at each time step and in turn receives a random impulse  $\mu$ . Notice that although the model (5) is not completely realistic, since it implies a discontinuous acceleration, it is physically much more acceptable than a Markovian model for the particle position  $x(t)$ , which would imply a discontinuity on the velocity field. The time scales over which the velocity is correlated are in fact much longer than the time scales of the acceleration and are determined by the largest eddies.

The solutions of (5) are well known and are characterized by variance and autocorrelation

$$\begin{aligned} \langle u \cdot u \rangle &= \sigma \\ R_L(\tau) &= \frac{\langle u(t) \cdot u(t + \tau) \rangle}{\sigma} = e^{-\tau} \end{aligned} \quad (6)$$

where  $\tau = t/T_L$ . The implications of (6) are that  $T_L$  is the integral time and that the statistics of  $x$  are characterized by

$$\begin{aligned} \langle x \cdot x \rangle &= \sigma t^2, & t \ll T_L \\ \langle x \cdot x \rangle &= \sigma T_L t, & t \gg T_L. \end{aligned} \quad (7)$$

TABLE 1. Parameters of Numerical Experiments

	Meander Amplitude, km	$K$ , $\text{cm}^2/\text{s}$	$\sigma$ , $\text{cm}^2/\text{s}^2$	$T_L$ , days	Comment
EXP0	70	$2.6 \times 10^6$	12.25	2.5	
EXPT1	70	$2.6 \times 10^5$	1.21	2.5	
EXPT2	70	$2.6 \times 10^5$	1.96	1.5	
EXPA1	40	$2.6 \times 10^6$	12.25	2.5	
EXPA2	100	$2.6 \times 10^6$	12.25	2.5	
EXPGM	$50e^{\Gamma t}$	$2.6 \times 10^6$	12.25	2.5	$\psi$ modified so jet has constant width

Equations (6) and (7) describes the classical results of Taylor [1921] for dispersion in a homogeneous turbulent flow. Notice that a limitation of the model (5) is that the autocorrelation function has a fixed exponential form (6). This limitation is not severe, however, since the exponential form appears to be general for homogeneous flows, independent of their spectrum shapes [Davis, 1991].

The archetype equations (5) can be generalized to include flows at higher dimensions, with mean shear and inhomogeneous and nonstationary turbulence. In this paper we apply the general formulation proposed by Thomson [1987] to the case of a two-dimensional homogeneous turbulent flow superimposed on the meandering jet  $U$ . The assumption of homogeneity is not very realistic, since the turbulent activity is likely to be different in various regions of the jet, but it provides a valid starting point for our process study.

In order to write the model equations in a compact way, we introduce the following notation: the velocity components  $u$ ,  $v$  and  $U$ ,  $V$  are indicated as  $u^i$  and  $U^i$ , respectively (with  $i = 1, 2$ ), and the particle coordinates  $x$ ,  $y$  are indicated as  $x^i$ . The model equations with this notation are

$$\begin{aligned} du^i &= -(F^{ij}u^j)dt + d\mu^i, \\ dx^i &= (U^i + u^i)dt, \end{aligned} \quad (8)$$

where  $\mathbf{F}$  is a constant tensor containing the information on the inverse of the time scales of the particle motion,  $d\mu^i$  is a random vector from a multivariate normal distribution with zero mean and second-order moments  $\langle d\mu^i \cdot d\mu^j \rangle = (T^{ik} \cdot \sigma^{kj} + T^{jk} \cdot \sigma^{ki})dt$ , and  $\sigma$  is a constant tensor containing the covariances of the fluid.

Notice that although (8) appears as a straightforward generalization of (5), the equations are now nonlinear, since  $U^i$  are nonlinear functions of  $x^i$ . If an inhomogeneous turbulent flow  $\sigma(x^i)$  was considered, a term  $(\partial\sigma^{ij}/\partial x^l)dt$  would be added to the right of (8). This term represents the velocity bias due to the gradient of the velocity covariance. Without this term the model would produce a (physically unrealistic) convergence of particles in the less energetic regions of the fluid, where the velocity covariance is lower.

We close this section by remarking that other formulations can be used to study particle diffusion. The most common is the equation of advection and diffusion

$$\partial C/\partial t = -U \cdot \nabla C + \nabla(K\nabla C)$$

where  $K$  is the space-dependent turbulent diffusivity. This equation can be derived as a special form of the equation for  $C$  associated with (4), valid for weakly inhomogeneous and stationary flows. In our problem, since the flow is strongly

inhomogeneous owing to the presence of the meandering jet, formulation (4) appears to be more appropriate. Notice that more elaborate and general forms of the advection and diffusion equation have been derived in the literature [e.g., Davis, 1987]. An interesting point that will be addressed in future studies is to compare limitations and performances of these more general equations for  $C$  with the Lagrangian method used here.

#### 4. NUMERICAL EXPERIMENTS

Six numerical experiments based on simulations of particle trajectories obtained by integrating (8) are presented. In all the experiments the turbulent field is assumed to be homogeneous and isotropic, so that only two turbulent parameters are needed, the variance  $\sigma$  and the time scale  $T_L$ . The basic experiment, EXP0, describes the diffusion processes in a turbulent field superimposed on the meandering jet (1) with the parameters given in section 2. Variations of the turbulence and meander parameters are treated in EXPT1 and EXPT2 and in EXPA1 and EXPA2, respectively. The last experiment, EXPGM, considers the case of a growing meander. The characteristics of the six experiments are reported in Table 1. The values for the turbulent parameters are suggested by experimental measures of small-scale turbulence in the Gulf Stream or in similar current systems, based on both measures of integrated fluxes of quasi-conservative tracers [Bower *et al.*, 1985; Olson, 1986] and direct observations of small-scale phenomena [Schmitt and Georgi, 1982]. The measurements do not provide a direct estimate of  $\sigma$  and  $T_L$ , but they provide indications that the turbulent diffusivity  $K$  ranges between  $10^5$  and  $10^6 \text{ cm}^2 \text{ s}^{-1}$ . From the value of  $K$  a rough estimate of  $\sigma$  and  $T_L$  can be made, assuming that the relationship  $K \approx \sigma T_L$  holds (notice that the estimates obtained in this way are probably a little high, since the experimental  $K$  is indeed an effective  $K$  for the system).

In theory, since the jet is highly inhomogeneous, for a complete description of the diffusion processes, the concentration  $C$  should be computed for all possible initial conditions. In practice, from the analysis of the deterministic velocity field given in section 2, we know that there are two different types of particle motion in the absence of turbulence, and we expect that a similar behavior will hold with turbulence. Initial conditions are therefore chosen in representative points of the recirculating and jet core regions discussed above. The validity of the choices of launch points were tested in EXP0, considering 10 points equally spaced along a section of the meander crest (Figure 1a) (lines along

TABLE 2. Time Scales and Péclet Numbers for Numerical Experiments

	Region	$T_a$ , days	$T_d$ , days	$P_e = \frac{T_d}{T_a}$
EXP0	Recirculation	20	218	11
	Jet core	8	50	6
EXPT1	Recirculation	20	2180	109
	Jet core	8	500	62
EXPT2	Recirculation	20	2180	109
	Jet core	8	500	62
EXPA1	Recirculation	20	70	3.5
	Jet core	6.5	110	17
EXPA2	Recirculation	20	445	22
	Jet core	9	18	2

other sections of the jet were studied but are not discussed here). In the discussion of the results of the experiments, we will refer mainly to two points, A in the recirculating region and B in the jet core region (Figure 1a).

In order to characterize the diffusion processes in the two regions, we have computed the Péclet number, which measures the relative strength of turbulence diffusion versus large-scale advection:  $P_e = T_d/T_a$ , where  $T_d$  is the diffusive time scale and  $T_a$  is the advective time scale.  $T_a$  is estimated as the average period of a particle in the absence of turbulence  $T_p$  in the two regions.  $T_d$  is estimated from  $T_d \approx L^2/K$ , where  $L$  is a representative length scale. For the recirculating regions,  $L$  is taken as the amplitude of the meander; for the jet core region,  $L$  is taken as the amplitude of the cross-stream section. The values of the time scales and the Péclet numbers are shown in Table 2 for five of the experiments. We have not computed the Péclet numbers for EXPGM because the representative scales cannot be determined when the meanders are growing in time.

All the experiments have been performed simulating the motion of 2000 independent particles for each initial condition in order to satisfactorily resolve the evolution of  $C$  in space. The time step  $dt$  used to integrate (8) was chosen small enough that the trajectory of the particle was consistent but large enough to be computationally reasonable. In all the experiments except EXPGM, the numerical integration for each initial condition was carried out for approximately 80 days, corresponding to  $2.5 T_m$ , the meander period. In EXPGM the simulation was run for only 20 days, corresponding to the doubling time for the meander amplitude.

#### 4.1. EXP0

In experiment EXP0, the stream function (1) with the parameters given in section 2 is used to describe the jet. The turbulence is characterized by the parameters  $\sigma = 12.25 \text{ cm}^2 \text{ s}^{-2}$  and  $T_L = 2.5$  days, corresponding to  $K = 2.6 \times 10^6 \text{ cm}^2 \text{ s}^{-1}$  (Table 1). The Péclet numbers (Table 2) are  $P_e = 11$  for the recirculating regions and  $P_e = 6$  for the jet core region, indicating that the balances in the two regions are quite similar and that diffusion is smaller than the advection.

*Diffusion from point A in the recirculating region.* The initial evolution of the concentration of the 2000 independent particles deployed at A is illustrated in Plate 2. Four snapshots of  $C(x, y)$  taken during the first 17 days at approximately 4-day intervals, are shown. Seventeen days is ap-

proximately the period  $T_p$  of a particle deployed at A in the absence of turbulence (hereafter indicated as the “deterministic particle”). The solid lines in Plate 2 represent the streamlines bounding the region of the jet where  $U > c$ , the open circles show the positions of the center of mass of the cloud of particles, and the asterisks show the positions of the deterministic particle, used as a reference to represent the purely advective motion. At 17 days only a reduced core of concentration has followed the deterministic particle as it completes its circuit. The remaining particles are left homogenizing in the meander bend. Figure 2 shows the percentage of particles between different values of  $\psi$  for the same times as Plate 2. The solid bars show particles approximately in the region  $U < c$ . The high percentage in this low-velocity region at day 17 is again very noticeable. The decrease in the tendency for the cloud to follow the deterministic particle can also be seen in Figure 3a, where the asterisks show the positions of the deterministic particle and the open circles show the trajectories of the centers of mass of the stochastic particles. As the deterministic particle moves across the streamlines inside the jet, for the first few days the center of mass follows it closely, but once the deterministic particle leaves the jet and slowly recirculates westward, the two trajectories diverge as the concentration starts to diffuse. After the first period the center of mass trajectory does not show any more oscillations but moves downstream with mean velocity  $c$  and maintains a constant  $y$ .

After 80 days, at the end of the integration, 65% of the particles are still in the initial recirculating region and have homogenized in it. The remaining particles have moved further downstream, often being trapped in other recirculating regions. Few particles, about 5%, at  $t = 80$  days are lost to the far field, defined as the area in which the jet has no influence on the velocity of the particle (140 km to the north and to the south of the center of the jet averaged along one wavelength).

*Diffusion from point B in the jet core region.* Plate 3 shows the evolution of the concentration in  $x$  and  $y$  of the particles deployed at B for the same period ( $t = 17$  days) as for Plate 2. The period of the deterministic particle with initial condition at B is  $T_p = 7$  days, so that the deterministic particle goes through more than two cycles in this figure. It is clear from an inspection of Plate 3 that the diffusion patterns are dramatically different from those obtained for point A. Particles now tend to be advected downstream in the jet but are lost in plumes that detach from the trailing edges of crests and troughs, corresponding to the points at which the advective motion of the deterministic particle is closer to the edges of the jet. By  $t = 8$  days, 8% of the particles are lost at the trailing edge of the first trough, and 35% are lost at the trailing edge of the next crest. The larger amount lost at this crest can be explained by the particle's initial position, which induces a deterministic motion closer to the edge of the jet in the crests than in the troughs (Figure 1b). There is, then, a higher probability of particles being lost from the northern extrema of the jet when the particles are affected by turbulence. Notice that because of the symmetry of the jet, the opposite pattern (more particles lost in the southern extrema) would occur for an initial condition close to the edge of a trough. At later times (12.5 and 17 days) and further downstream, smaller and smaller plumes are lost at the extrema, as there are fewer and fewer particles remaining in the jet. Figure 4 shows the corresponding

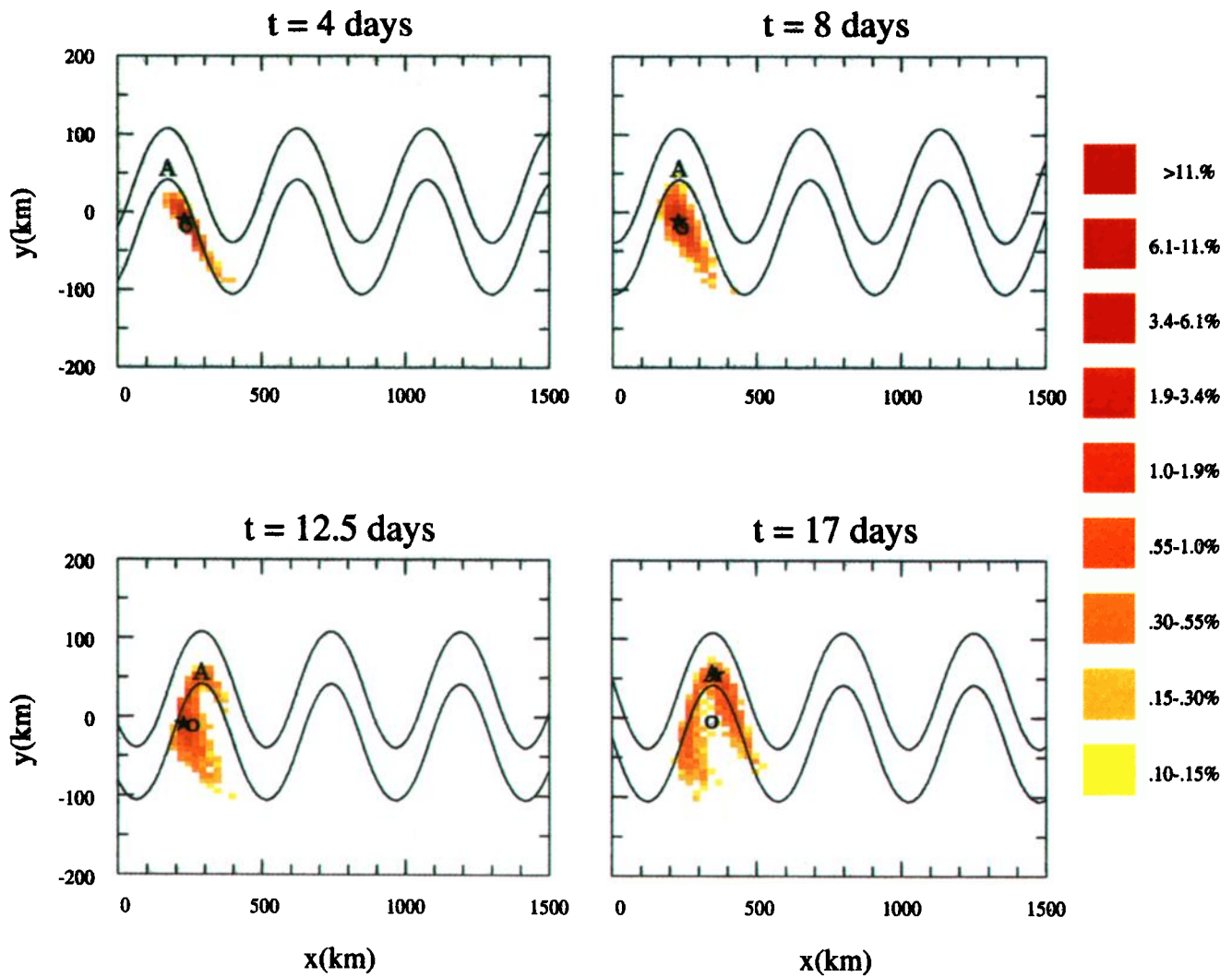


Plate 2. Initial evolution (17 days) of the concentration of particles in  $x$  and  $y$  for particles launched at A, in the recirculating region, in experiment EXP0. Solid lines represent streamlines in the fixed reference frame, stars represent the positions of the deterministic particle, and open circles represent the centers of mass of the clouds of particles. Concentration is determined by the percentage of particles in  $85\text{-km}^2$  bins. A logarithmic color scale is used, suggested by the distribution of the concentration in the 17 days.

histograms of the percentage of particles in intervals of  $\psi$ . Although large numbers of particles are lost in plumes, most of them do not leave the region of influence of the jet but are caught in recirculating regions where they are reentrained and recirculate, slowly being homogenized. For example, at 80 days, 15% of the particles are still in the second recirculation region, compared to 35% there at 8 days. An important consequence of the trapping of particles in the recirculation regions is the slowing down of the downstream transport, as indicated by the trajectory of the center of mass (Figure 3b). The percentage of particles lost to the far field is approximately 18%. The increase over that found for point A is caused by the fact that particles are lost from the extrema of the meanders and thus have a greater probability of moving further north or south beyond the influence of the jet.

Some aspects of the diffusion patterns can be understood in terms of the known theory of shear dispersion. For instance, the local tendency toward homogenization inside the recirculation regions is a well-known phenomenon [Rhines and Young, 1982; Dewar and Flierl, 1985]. On the

other hand, the understanding of the complete system, with the trapping of particles from the core into the recirculation regions, is more complex. Systems of this type (although usually with closed boundary conditions) have been studied in various fields of physics in the context of the theory of "anomalous diffusion" [e.g., Young and Jones, 1991]. They are characterized by a "holdup" of particles (or tracer) in trapping regions that determines a modification of the downstream dispersion with respect to the case of pure shear dispersion [Taylor, 1953]. Typically, the downstream dispersion averaged over a cross-stream section turns out to be proportional to  $t^\nu$ , with  $\nu \neq 1$ . The exponent  $\nu$  can be theoretically computed a priori in some special cases [Young, 1988; Young et al., 1989]. Although a theoretical analysis of this type for the dispersion of our system goes beyond the purpose of this paper, it is a very interesting topic and will be considered in future research.

To conclude, we mention the results from simple statistics that can easily be compared with observations. Using the results from the 10 initial conditions on the cross section in

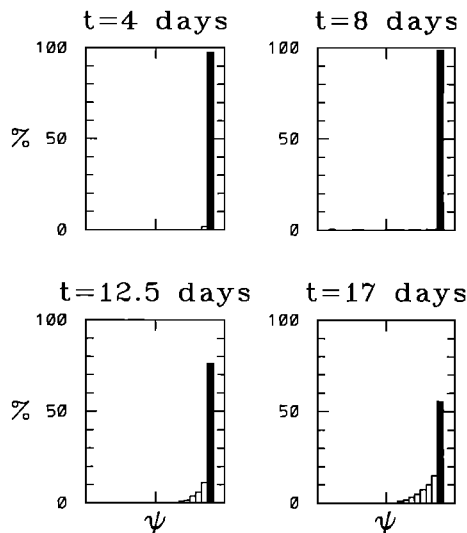


Fig. 2. Histograms of percentages of particles in intervals of  $\psi$  in the fixed reference frame for experiment EXP0. Shaded bars show particles out of the jet.

Figure 1a, we compute the percentage of particles leaving the region where  $U > c$  at least once during the first wavelength  $\lambda$  after deployment. We find that about 75% of the stochastic particles, i.e., virtually all the particles deployed in the recirculating region and about half of the particles deployed in the jet core region, leave the jet during the first  $\lambda$ . In comparison, *Bower and Rossby* [1989] found a percentage of approximately 60% from the analysis of RAFOS data. Although the statistics from the data is obtained from only 30 floats and their initial conditions are different from the idealized ones that we consider, the smaller percentage found by Bower and Rossby suggests that the turbulent flow might be too vigorous in our experiment or that the jet core region might be too narrow. In the following experiments we will consider the effect of reducing turbulence and varying the jet parameters that determine the ratio of the width of the jet core region to the meander amplitude.

#### 4.2. Effects of Reducing $K$ and Changing Meander Amplitude

The effects of changing the turbulence parameters are studied in EXPT1 and EXPT2. In both cases  $K$  is reduced to  $2.6 \times 10^5 \text{ cm}^2 \text{ s}^{-1}$  but with different values of  $\sigma$  and  $T_L$  (Table 1). The results of the two experiments are very similar, showing that  $K$  is a rather good comprehensive parameter for turbulence. With respect to EXP0, the results are qualitatively similar, but because of the reduced turbulence, the process of homogenization is slowed down in the recirculation regions and the particles are lost in smaller plumes from the core region. Approximately 60% of the particles (as opposed to the 75% of EXP0) are found to leave the  $U > c$  region at least once within the first wavelength.

Changes in one of the jet parameters are considered in EXPA1 and EXPA2. The meander amplitude  $A$  is chosen to be 40 km in EXPA1 and 100 km in EXPA2, while the turbulence parameters are kept as in EXP0 (Table 1). Again, the qualitative diffusive patterns are the same as in EXP0,

but the number of particles lost in plumes from the core increases with increasing  $A/W$  (where  $W$  is the jet width). *Bower* [1991] has shown that the ratio  $A/W$  determines the ratio between the areas of the jet core and those of the recirculation regions in the moving frame, with the jet core area decreasing with increasing  $A/W$ . This means that if deterministic particles are launched along a jet cross section in the fixed frame, with increasing  $A/W$  there is a decrease in the fraction of particles which flow downstream without exiting and reentering the jet (*Bower* [1991] calls this the "transport in the jet alone"). Our results show that this fraction decreases even faster with increasing  $A/W$  in the presence of turbulence. As the jet core becomes narrower, in fact, not only does it contain fewer particles, but also the particle's probability of escaping from it increases. The percentages of particles leaving the jet within the first wavelength are approximately 45% for EXPA1 and 90% for EXPA2.

#### 4.3. Effects of Growing Meanders

In the EXPGM experiment the turbulent motion of particles is studied in the presence of time-dependent, growing meanders. Only the initial evolution of the meanders is considered, and the growth is modeled in an exponential fashion with a doubling time of 20 days (20 days is also the duration of the experiment). The jet model is modified with respect to (1) in order to minimize an increase in the velocity as a consequence of the growth term. This is done by incorporating a normalization factor [*Bower*, 1991] in (1) that

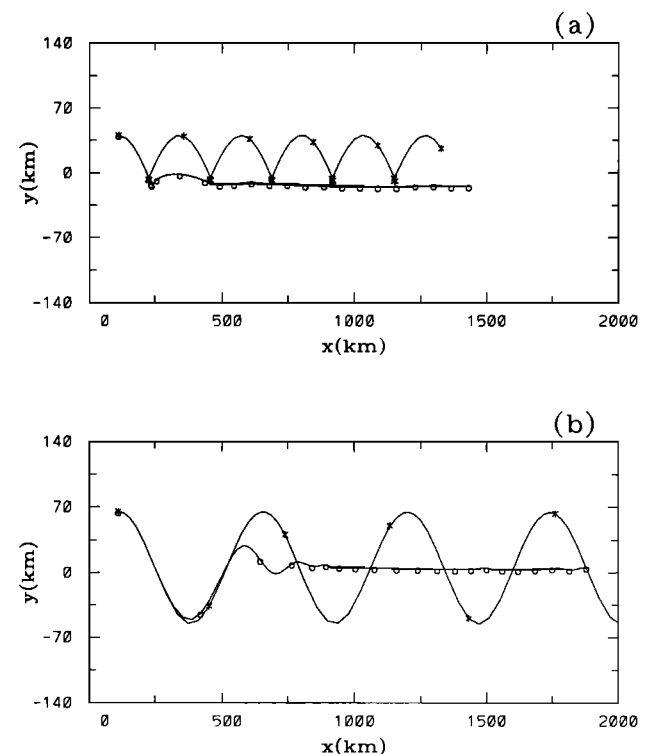


Fig. 3. Trajectory of deterministic particle (asterisks) and center of mass of cloud of stochastic particles (open circles) for experiment EXP0. Asterisks and open circles are plotted every 100 hours. (a) Particles launched in recirculating region; (b) particles launched in jet core region.

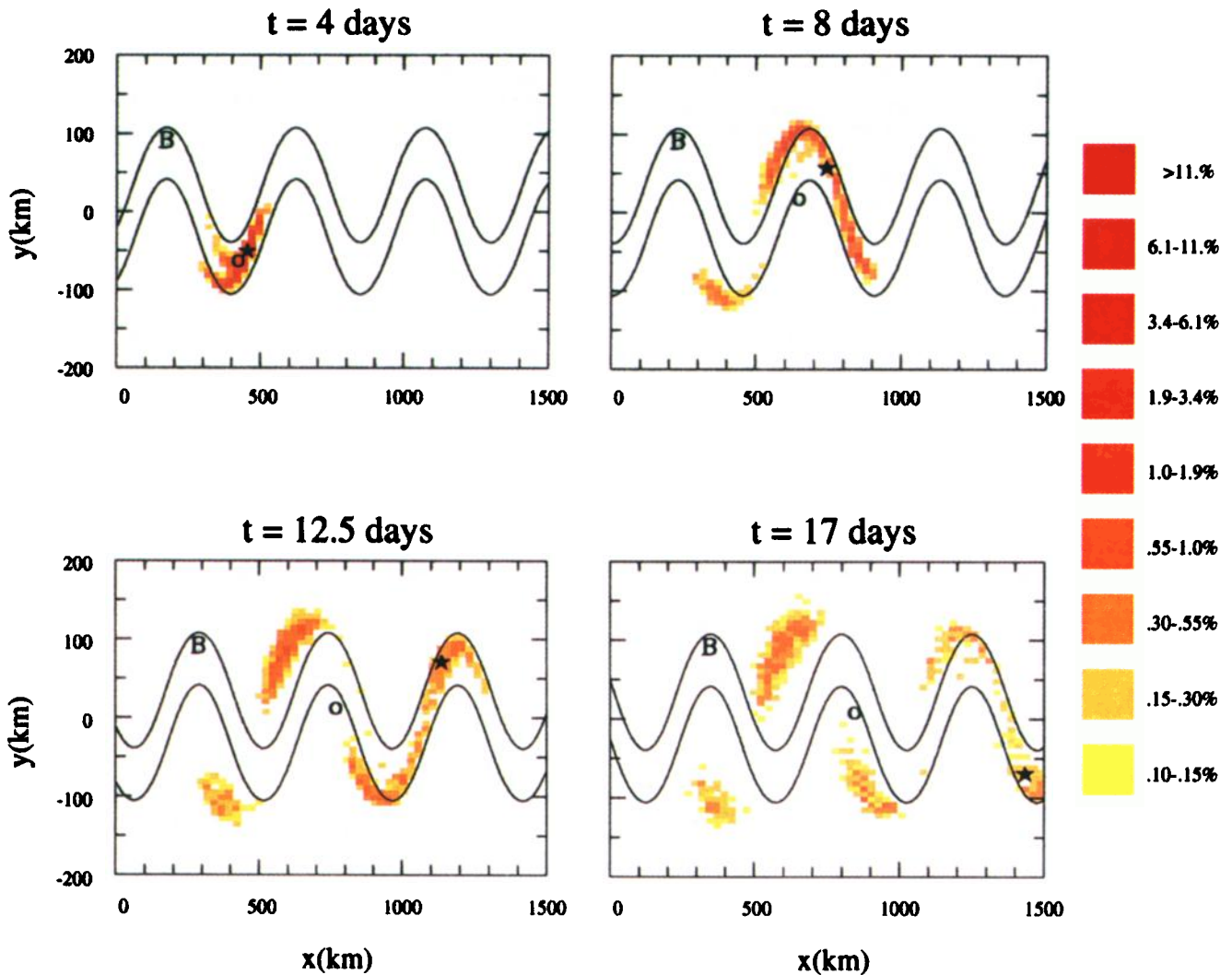


Plate 3. Evolution of concentration of particles launched at B, in the jet core region, for experiment EXP0 (see Plate 2).

maintains an approximately constant jet width. The jet width is slightly greater than in EXP0 ( $W = 80$  km), but the turbulent parameters are the same (Table 1).

The results of EXPGM can be summarized as follows. Particles launched in the jet core region appear to be lost in increasing numbers in plumes, while the meander grows. The majority of the particles are caught in the recirculating regions and tend to remain trapped in them, but they are not homogenized as efficiently as in the previous experiments with fixed amplitude after 20 days. As the amplitude grows, more streamlines tend to close, but this increase occurs faster than the dispersion of particles across the streamlines, so particles remain in the apex of the recirculating region. In conclusion, the growth of the meanders seems to enhance the exchange between the jet core region and the recirculating regions, but the homogenization in the recirculating regions is slowed down.

The differences between the steady and growing meander can be visualized by qualitatively comparing the motion of particles launched in the jet core in EXP0 (Figure 3b) with that of particles in EXPGM (Figure 5a) and by considering

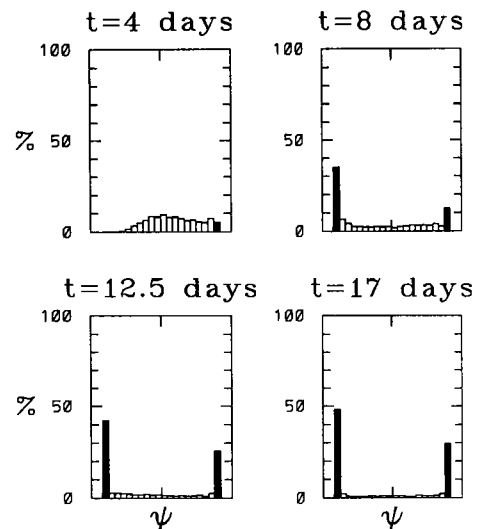


Fig. 4. Histogram of percentage of particles in intervals of  $\psi$  for particles launched at B, in the jet core region, for experiment EXP0 (see Figure 2).

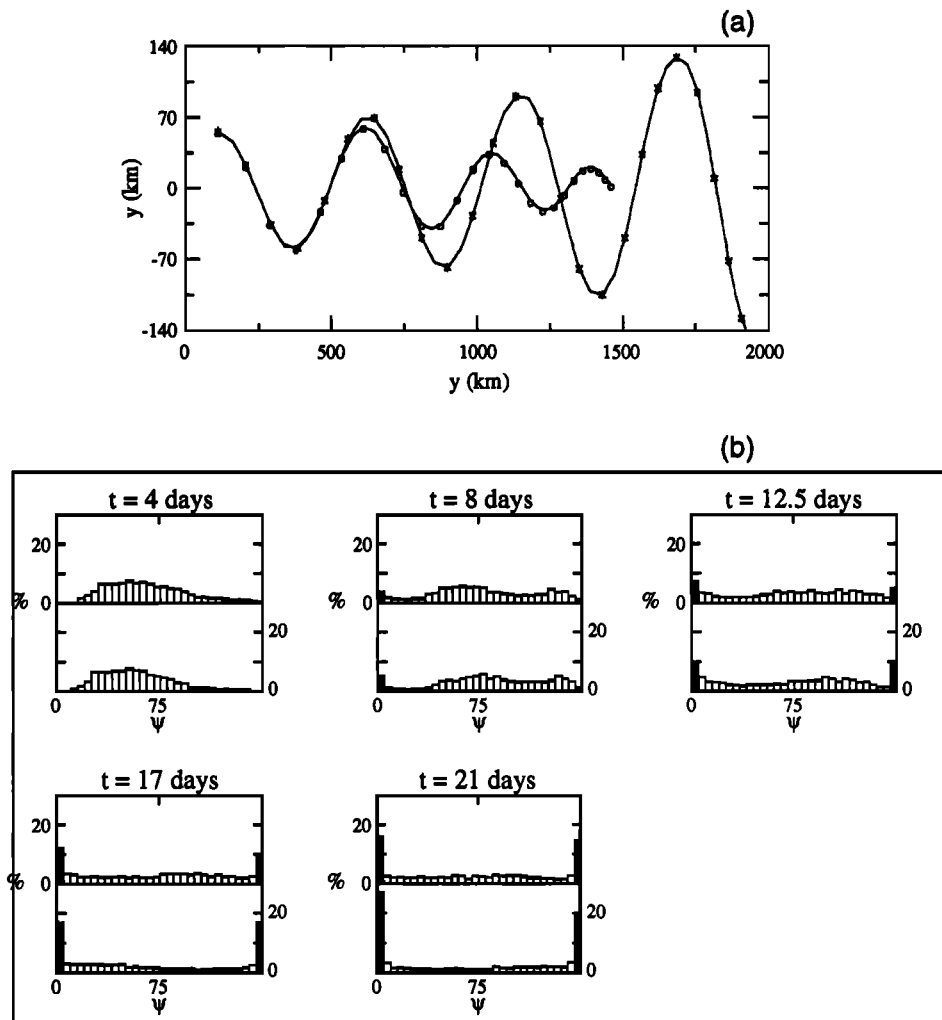


Fig. 5. (a) Trajectory of deterministic particle (asterisk) and center of mass of cloud of stochastic particles (open circles) for experiment EXPGM. Asterisks and open circles are plotted every 20 hours for particles launched in the jet core region. (b) Histograms of percentage of particles in intervals of  $\psi$  for particles launched at B, in the jet core region, (bottom) for experiment EXPGM and (top) for the same stream function without the growth of the meanders. Shaded bars show particles out of the jet. Note that even in the case of no growth, the results do not compare to EXP0, since a different  $\psi$  with smaller meander amplitude ( $A = 50$  km) and greater jet width ( $W = 80$  km) is used.

the histograms in Figure 5b. The deterministic path in Figure 5a shows that the deterministic motion alone in EXPGM increases the excursion of a particle launched at point B, but it does not expel the particle from the core region (this can be seen by comparing the particle position with the meander amplitude). The center of mass of the ensemble of particles with turbulence exhibits protracted oscillations in the growing-meander case. This is directly tied to the influence of meander amplitude change, i.e., the deterministic influence of the jet and its impact on the particles expelled from the jet core to the recirculation regions. The histograms in Figure 5b show that the meander growth changes the positions of modes and the occupation of the extreme stream function intervals. The central stream function intervals are depleted of particles faster, while the effect of the constant meander is to make the particle concentration uniform across the jet.

EXPGM is the only experiment in which time-dependent meanders are considered. This time dependence can lead to

a mechanism of deterministic dispersion [Samelson, 1992] in addition to the stochastic dispersion. Sorting out the effects of the two mechanisms quantitatively is not easy, mainly because the experiment has not been run for enough time nor enough initial conditions to define the nature of the deterministic motion. Nevertheless, it seems reasonable to hypothesize that the observed increased exchange between core and recirculation regions is due to both mechanisms. Overall, our results agree with those of Samelson [1992], who also found increased mixing tied to low-frequency changes in meander amplitude. The tendency to isolate this effect to the exchange between the jet core and the recirculation region is also consistent with his results. As pointed out by a reviewer, the subtle differences between the current simulations and those of Samelson [1992] are harder to quantify because of the differences in the deterministic fields used. More detailed analysis on dispersion mechanisms in the presence of a time-dependent field should be carried out using dynamical models, where the meander growth is

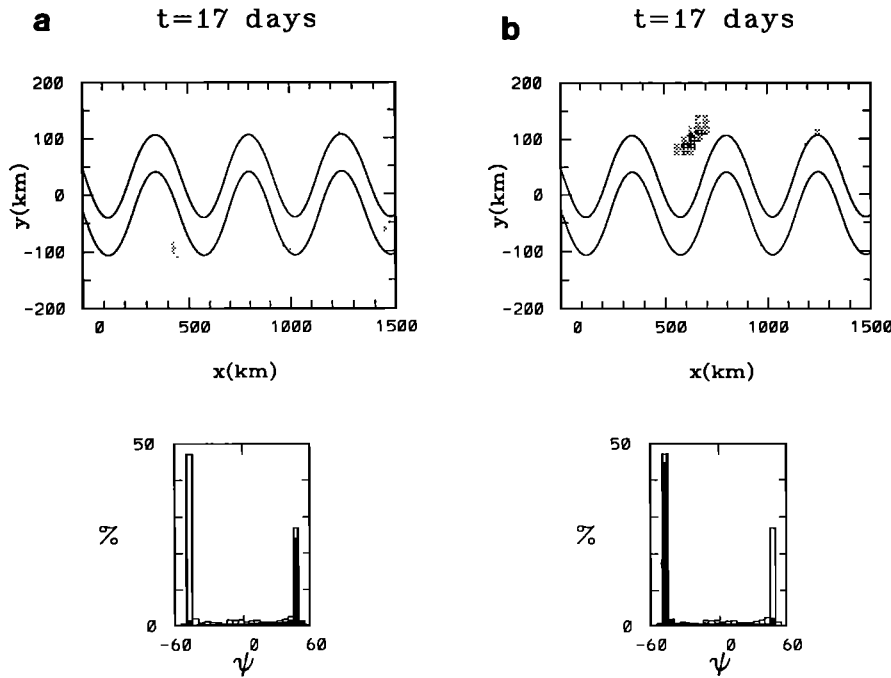


Fig. 6. Distribution of species in parcels initialized at position B (in the jet core). Shaded areas of histograms show percentage of the total possible population. (a) Southern species; (b) northern species.

related to instability mechanisms and is dynamically consistent [e.g., Lozier and Bercovici, 1992].

5. APPLICATION TO CROSS-STREAM SPECIES DISTRIBUTIONS

In this section each of the particles in the simulations above is treated as a small component of the ecosystem. Each particle contains a mixture of species that will undergo various environmental perturbations as they are advected and diffused along the jet. As above, the simulation is an ensemble of particles and does not allow particle-particle interaction. In keeping with the basic idea of considering the effects of diffusive perturbations on a deterministic field, the effect of the environment on each of two species is assumed to be a function of the deterministic stream function. A simple logistic form involving competition for a constant resource  $\kappa$ , which represents nutrients or food but with differential ability to utilize the resource, dependent on  $\psi$ , is assumed [cf. Murray, 1989, for a detailed discussion]. Therefore the two species are adapted for either side of the stream and have equal growth potential at the center of the jet.

The growth of a population of the  $i$ th species along a trajectory is then given by

$$dN_i/dt = \alpha_i(\psi)(\kappa - N_s)/\kappa - \gamma N_i; \quad i = 1, 2$$

where  $N_s$  represents a sum of both species and  $\gamma$  is a linear loss term. The functional dependence of  $\alpha_i(\psi)$ , the growth rates, are assumed such that

$$\alpha_i(\psi) = \alpha_o \left| \left( 1 + \frac{\psi}{\psi_i^0} \right) \right|$$

where  $\psi_i^0$  represents the preferred environment for the  $i$ th species. These are respectively set for the minimum (northern species) and maximum (southern species) stream functions. Note that  $\psi = 0$  at the center of the jet. In the

simulations the jet and turbulent parameters are the same as in EXP0. Two thousand parcels are initialized at points A and B. Each parcel is started with equal numbers of each species. The trajectory of each parcel is then followed, with calculations made at each time step of the abundance of each species. Figure 6 shows the results after 17 days for the case of parcels launched at B. (It is useful to consider these figures in comparison to Plate 3.) Figure 6a shows the abundance of southern species, and Figure 6b shows the abundance of the northern species. It is obvious that the biological interaction is strongly modified by the motion of the parcels into different environments as specified by the stream function. Consideration of the histograms of populations on  $\psi$  show the patches which form in the meander recirculation regions to be dominated by the species with an affinity to that side of the jet. For example, the northern species dominates in the meander trough, while the southern species has higher population levels in the recirculation region associated with the meander crest. If one considers this against the optimal population level which would exist in the absence of competition, however, there is a diminution of favored species in the patches. While the cross-jet trends in population density in the histograms are approximately linear, there is an increase in the expatriate population from opposite sides of the jet in the patches in the recirculation regions. That is, their population level exceeds that expected from the linear trend in the histograms across the stream function values in the stream core. Therefore the patches in meander crests and troughs do maintain an expatriate population as a direct response to cross-jet axis transfer. The existence of these populations in patches from the opposite side of the jet depends on the ratio of the rate of competitive exclusion to the diffusive source. Results for parcels initialized at A show the expected tendency for the northern species to diminish and the southern species to thrive within

the initial recirculation region to the south of the jet. It is the portion of the population initially from the jet core, then, that is responsible for patches of mixed populations appearing on either side of the jet. This patchiness is maximum in proximity to crests and troughs in the recirculating fluid.

## 6. CONCLUSIONS

The major contribution of this work is the inclusion of small-scale turbulence in the kinematic simulation of float trajectories in a meandering jet. As such it is an extension of the results of *Bower* [1991] and *Samelson* [1992]. The problem of small-scale turbulence is approached as a Markov process with parameters  $\sigma$  and  $T_L$ , the variance and the time scale, respectively, of the turbulent velocity field. From  $\sigma$  and  $T_L$ , a diffusivity parameter  $K \approx \sigma T_L$  can be estimated; it appears to be robust.

The influence of the turbulent diffusion on the distribution of particles depends upon the region into which the particles are originally introduced, i.e., the jet core, the recirculating region, or the far-field region of the stream function as viewed in the translating frame. Particles in the recirculating region tend to be trapped in it, and the effect of the turbulence is to homogenize them within the closed stream function [*Rhines and Young*, 1982; *Dewar and Flierl*, 1985]. The center of mass is moved to the south of the jet mean for anticyclonic recirculating regions (meander crests, high  $\psi$ ) and to the north for the cyclonic counterparts (troughs, low  $\psi$ ). Particles deployed in the jet core region tend to cross boundaries into the recirculating regions. This occurs along a local axis of deformation in the flow field in proximity to the crests and troughs. This process produces a chain of particle patches entrained into the recirculation regions as the overall cloud of particles passes downstream, with the concentration in the consecutive trapped regions decreasing downstream. The trapping of particles in the recirculation regions is suggestive of an "anomalous diffusion" behavior of the system. The exchange with the far field is small and depends entirely on the diffusion and is therefore limited in extent for the short integration times here.

With respect to the model of *Bower* [1991], the introduction of turbulence allows the particles to cross streamlines in the translating frame, resulting in the homogenization inside closed recirculation regions and in the large exchange between the core and the recirculation regions described above. The mechanism of exchange between regions studied here is different from the one considered by *Samelson* [1992]. In *Samelson's* model there is no turbulent field, but the large-scale flow is allowed to change in time. The time dependence induces breakings in the boundaries between regions and this in turn allows particle exchange. Notice that the particles considered by *Samelson* are strictly deterministic and that the flux between regions is computed for a specific representation of the flow. The flux that we consider, instead, is averaged over representations and therefore describes only the behavior of the mean particle concentration. Since each particle is considered independently, we do not need to specify the spatial structure of the turbulent field. The frequency spectrum is chosen to be appropriate for small-scale Lagrangian turbulence, approximately white for frequency  $\omega$  lower than the frequency corresponding to the Lagrangian time scale  $T_L$ , and decreasing as  $\omega^{-2}$  for higher frequency. *Samelson*, on the other

hand, considers large-scale fluctuations harmonic in time. Despite these differences, it is interesting to compare our results with those of *Samelson*. A large exchange between the core and the recirculation regions, especially in relation to the fluctuations of the meander amplitude, is also found by *Samelson*. A combination of the two mechanisms, turbulent mixing and time dependence, is expected to take place in realistic flows (a simple example is studied here in relation to meander growth). *Samelson* also finds a noticeable exchange between the recirculation regions and the far field, something we do not find. As noted above, the small exchange in our model is due to the lack of shear enhancement in the diffusion outside of the stream. The purely diffusive time scales are much longer than the ones considered here. Finally, the results of *Samelson* suggest very little exchange across the center of the jet, at least in the case of fluctuating meanders. This is not surprising, since in order to have cross-jet mixing [*del Castillo-Negrete and Morrison*, 1993], the recirculating regions from different modes of oscillation have to overlap across the jet center so that the central barrier breaks and particles are allowed to cross the jet center. This is expected to occur if the recirculating regions are very large, which implies very large meander amplitudes. In our model, instead, cross-jet mixing occurs also for moderate amplitude (although mixing increases with increasing amplitude), because the stochastic turbulent motion allows particles to cross dynamical regions even if they do not break.

The buildup of homogenized particle distributions in the trapped regions has important ramifications in terms of biological patchiness. Since the time particles spend in these regions is long compared to the reproduction time of phytoplankton and microzooplankton, it can be argued that these regions are a major source of patchiness in the Gulf Stream and similar currents. A simple biological model has been incorporated in our kinematic model, with the Gulf Stream acting as a barrier between species and with one variety dominating the Slope Water and another one dominating the Sargasso Sea. The model shows the observed tendency to produce patches of species in the recirculation regions on the side of the stream each species favors.

To explore the picture of particle distributions gained from the kinematic simulations, a short run of a meandering jet in a primitive equation channel model is presented (Figure 7). The model is the *Bleck and Boudra* [1986] isopycnal code configured to a zonal channel. The model has three isopycnal layers which are chosen in a manner that approximates the two-layer results of *Ikeda and Apel* [1981]. The model is initialized with a linear jet and a small perturbation. The result is a growing meander pattern as shown in Figure 7. Particles launched in the core of the jet slowly diffuse out as they are advected into the first meander trough. At the trough a portion of the particles diffuses into a developing recirculation region and is trapped. Other particles proceed into the next meander crest. These occurrences are reminiscent of the kinematic simulations. The major difference between the kinematic simulation and the primitive equation model involves the details of the evolution of the flow field. To some extent this evolution follows the tendencies observed in the particle distributions; i.e., the kinematic simulation provides a partial rationale for describing the development of the height field seen in the model. While any detailed treatment at longer time scales needs to be con-

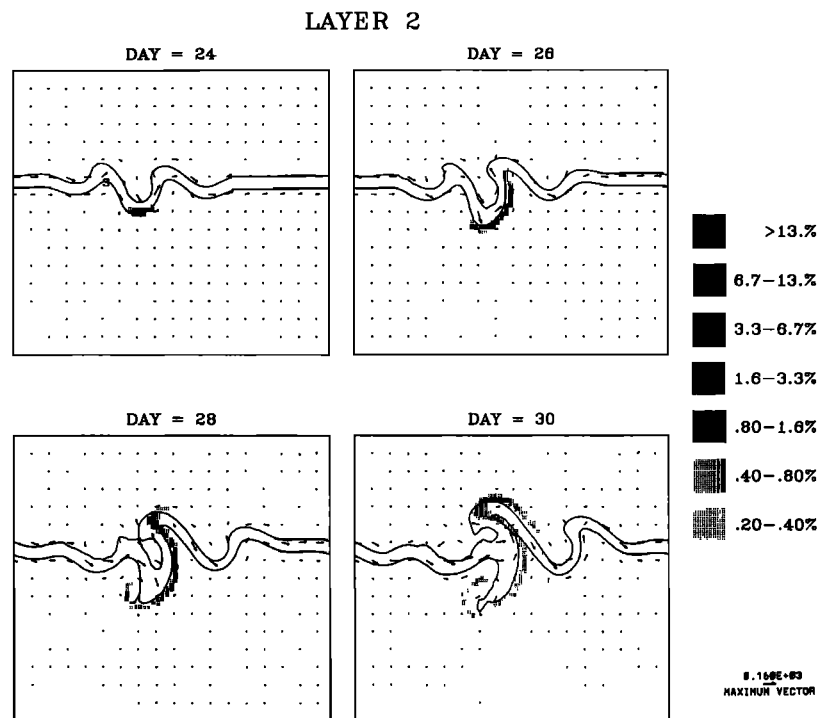


Fig. 7. The primitive equation isopycnal model of *Bleck and Boudra* [1986] in a zonal channel configuration was used to analyze the evolution of the concentration of particles launched in the core of the dynamic jet. Spatial resolution is 20 km. Particles were launched at a single point  $s$  on the jet at day = 20. Solid lines indicate depth field lines, and arrows show velocity vectors at every four grid points. Concentration is determined by percentage of particles in 400-km<sup>2</sup> bins. A logarithmic shading scale is used. As in the kinematic model, the concentration here gives ensemble-averaged diffusion.

cerned with the difference between passive and active tracers, the conclusion is that the simulation does indeed provide a realistic depiction of the meandering stream.

**Acknowledgments.** The authors would like to thank Peng Ge for providing the results from the dynamic model. We would also like to thank Horacio Figueroa for the Lagrangian code used in both the kinematic and dynamic models and Geoff Samuels for the satellite image (the data for which were collected as part of BIOSYNOP by the University of Miami remote sensing group). Comments from Amy Bower and Glenn Flierl proved to be very useful. This work was supported by the National Science Foundation (grant OCE9102604) and by the Office of Naval Research (grants N00014-89-J-1536 (BIOSYNOP) and N00014-91-J-1346). This work is part of an undergraduate honor thesis that was initially supported by an REU grant from the National Science Foundation (grant OCE8800135).

#### REFERENCES

- Backus, R. H., Biogeographic boundaries in the open ocean, in *Pelagic Biogeography*, UNESCO Tech. Pap. Mar. Sci., vol. 49, pp. 9-13, 1986.
- Bleck, R., and D. B. Boudra, Wind-driven spin-up in eddy-resolving ocean models formulated in isopycnic and isobaric coordinates, *J. Geophys. Res.*, **91**, 7611-7621, 1986.
- Bower, A. S., A simple kinematic mechanism for mixing fluid parcels across a meandering jet, *J. Phys. Oceanogr.*, **21**, 173-180, 1991.
- Bower, A. S., and H. T. Rossby, Evidence of cross-frontal exchange processes in the Gulf Stream based on isopycnal RAFOS float data, *J. Phys. Oceanogr.*, **19**, 1177-1190, 1989.
- Bower, A. S., H. T. Rossby, and J. T. Lillibridge, The Gulf Stream—barrier or blender?, *J. Phys. Oceanogr.*, **15**, 24-32, 1985.
- Cornillon, P., D. Evans, and W. Large, Warm outbreaks of the Gulf Stream into the Sargasso Sea, *J. Geophys. Res.*, **91**, 6583-6596, 1986.
- Csanady, G. T., *Turbulent Diffusion in the Environment*, 248 pp., D. Reidel, Norwell, Mass., 1980.
- Davis, R. E., Oceanic transport, Lagrangian particle statistics, and their prediction, *J. Mar. Res.*, **41**, 163-194, 1983.
- Davis, R. E., Modelling eddy transport of passive tracers, *J. Mar. Res.*, **45**, 635-666, 1987.
- Davis, R. E., Observing the general circulation with floats, *Deep Sea Res.*, **38**, suppl., S531-S571, 1991.
- del Castillo-Negrete, D., and P. J. Morrison, Chaotic transport by Rossby waves in shear flow, *Phys. Fluids A*, **5**(4), 948-965, 1993.
- Dewar, W. K., and G. R. Flierl, Particle trajectories and simple models of transport in coherent vortices, *Dyn. Atmos. Oceans*, **9**, 215-252, 1985.
- Flierl, G. R., Particle motion in large-amplitude wave fields, *Geophys. Astrophys. Fluid Dyn.*, **18**, 39-74, 1981.
- Grice, G. D., and A. D. Hart, The abundance, seasonal occurrence and distribution of the epizooplankton between New York and Bermuda, *Ecol. Monogr.*, **32**, 287-309, 1962.
- Hanna, S. R., Some statistics of Lagrangian and Eulerian wind fluctuations, *J. Appl. Meteorol.*, **18**, 518-525, 1979.
- Ikeda, M., and J. R. Apel, Mesoscale eddies detached from spatially growing meanders in an eastward-flowing oceanic jet using a two-layer, quasigeostrophic model, *J. Phys. Oceanogr.*, **11**, 1638-1661, 1981.
- Lambert, R. B., Lateral mixing processes in the Gulf Stream, *J. Phys. Oceanogr.*, **12**, 851-861, 1982.
- Langevin, P., Sur la théorie du mouvement brownien, *C. R. Seances Acad. Sci. Paris*, **146**, 530-533, 1908.
- Lozier, M. S., and D. Bercovici, Particle exchange in an unstable jet, *J. Phys. Oceanogr.*, **22**, 1506-1516, 1992.
- Monin, A. S., and A. M. Yaglom, *Statistical Fluid Mechanics*, vol. 1, 769 pp., MIT Press, Cambridge, Mass., 1971.
- Murray, J. D., *Mathematical Biology*, 767 pp., Springer-Verlag, New York, 1989.

- Olson, D. B., Lateral exchange within Gulf Stream warm-core ring surface layers, *Deep Sea Res.*, 33, 1691–1704, 1986.
- Owens, W. B., A synoptic and statistical description of the Gulf Stream and subtropical gyre using SOFAR floats, *J. Phys. Oceanogr.*, 14, 104–113, 1984.
- Pasquill, F., and F. B. Smith, *Atmospheric Diffusion*, 3rd ed., 437 pp., Halsted Press, New York, 1983.
- Rhines, P. B., and W. R. Young, Homogenization of potential vorticity in planetary gyres, *J. Fluid Mech.*, 122, 347–367, 1982.
- Samelson, R. M., Fluid exchange across a meandering jet, *J. Phys. Oceanogr.*, 22, 431–440, 1992.
- Schmitt, R. W., and D. T. Georgi, Finestructure and microstructure in the North Atlantic current, *J. Mar. Res.*, 40, 5659–5705, 1982.
- Taylor, G. I., Diffusion by continuous movements, *Proc. London Math Soc.*, 20, 196–212, 1921.
- Taylor, G. I., Dispersion of soluble matter in solvent flowing slowly through a tube, *Proc. R. Soc. London Ser. A*, 219, 186–203, 1953.
- Thomson, D. J., A random walk model of dispersion in turbulent flows and its application to dispersion in a valley, *Q. J. R. Meteorol. Soc.*, 112, 511–530, 1986.
- Thomson, D. J., Criteria for the selection of stochastic models of particle trajectories in turbulent flows, *J. Fluid Mech.*, 180, 529–556, 1987.
- van Dop, H., F. T. M. Nieuwstadt, and J. C. R. Hunt, Random walk models for particle displacements in inhomogeneous unsteady turbulent flows, *Phys. Fluids*, 28, 1639–1653, 1985.
- Wishner, K. F., and S. K. Allison, The distribution and abundance of copepods in relation to the physical structure of the Gulf Stream, *Deep Sea Res.*, 33, 705–731, 1986.
- Young, W. R., Arrested shear dispersion and other models of anomalous diffusion, *J. Fluid Mech.*, 193, 129–149, 1988.
- Young, W. R., and S. Jones, Shear dispersion, *Phys. Fluids A*, 3, 1087–1101, 1991.
- Young, W. R., A. Pumir, and Y. Pomeau, Anomalous diffusion of tracer in convective rolls, *Phys. Fluids A*, 1, 462–469, 1989.

S. Dutkiewicz, Graduate School of Oceanography, University of Rhode Island, Narragansett, RI 02882.

A. Griffo and D. B. Olson, Rosenstiel School of Marine and Atmospheric Science, University of Miami, Miami, FL 33149.

(Received June 2, 1992;  
revised May 17, 1993;  
accepted May 20, 1993.)